Supporting Information

Polymer Crystallization by Photochemical Dimerization of a PDMS Copolymer

Taylor Wright,[a] Yael Petel,[a] Carson O. Zellman,[c] Ethan R. Sauvé, [a] Zachary M. Hudson,[a] Carl A. Michal,[a,b] Michael O. Wolf*[a]

[a] Department of Chemistry, University of British Columbia, Vancouver, BC, Canada, V6T 1Z1

[b] Department of Physics and Astronomy, University of British Columbia, Vancouver, BC, Canada, V6T 1Z1

[c] Department of Chemistry, Simon Fraser University, 8888 University Drive, Burnaby, BC, Canada V5A 1S6

General Experimental Details

(6-7% Aminopropylmethylsiloxane) – dimethylsiloxane copolymer (AMS-163), M_n = 50,000 g/mol, was purchased from Gelest. All other reagents were purchased from Sigma Aldrich and used without further purification.

^{1}H NMR spectroscopic data was collected on a 400 MHz Bruker Avance 400dir spectrometer at 25 °C. ^{13}C NMR spectroscopic data was collected on a 600 MHz Bruker Avance 600cp spectrometer at 25 °C. Residual solvent peaks were used to reference the spectra. NMR spectra are reported in parts per million (ppm).

Mass spectrometry measurements were conducted on a Waters-ZQ instrument equipped with an ESCI/APCI ionization source. Elemental analysis measurements were performed on a Thermo Flash 2000 Elemental Analyzer.

Infrared spectra were collected on a PerkinElmer Frontier FT-IR with a diamond ATR plate. Absorption spectra were collected on a Varian Cary 5000 UV-Vis-NIR spectrophotometer.

Optical microscope images were collected on a Bruker Senterra II Compact Raman Microscope using a 10× magnification. Polarized optical microscopy images were collected on an Olympus BX53M using a linear polarizer and 530 nm retardation plate.

Fluorescence microscope images were collected on an Olympus IX83 Inverted Fluorescence Microscope equipped with a metal-halide lamp. An excitation wavelength of 350 nm was used with no filters applied to the emitted light.

Differential scanning calorimetry (DSC) measurements were performed using a TA Instruments DSC Q2000 instrument with a TA Instruments Refrigerated Cooling System 90 at a ramp rate of 10 °C/min.

PXRD measurements were collected on a D8-Advance instrument with a Cu source and LynxEye detector at room temperature.

Atomic force microscopy images were collected using an Asylum Instruments Cypher S AFM system operating in tapping mode or fast force mapping mode. Mikromasch HQ:NSC14/No Al or HQ:NSC19/No Al probes, with typical resonance frequencies f and spring constants k of (f = 160 kHz, k = 5 N/m) and (f = 65 kHz, k = 0.5 N/m) were used.

Confocal microscopy was performed on an Olympus FV1000 Laser Scanning Microscope using simultaneous reflectance, transmittance, and fluorescence (λ_{ex} = 360 nm) modes. Data was treated using the Volocity software package.

X-Ray scattering measurements were performed on a Ganesha 300XL+ instrument in transmission mode.

Solid-state PFG NMR experiments were performed on a home-built NMR spectrometer based on an Oxford Instruments 8.4 T wide bore magnet.[1] Liquid samples were transferred to an NMR tube and measured neat. Solid samples were irradiated as described below and then removed from the glass slide and packed into an NMR tube for measuring.

Synthesis

9-Anthracene-methylacetoacetate (**AnAc**):

9-Anthracenemethanol (1.5 g, 7.2 mmol), *tert*-butyl acetoacetate (2.51 mL, 14.4 mmol), and *m*-xylenes (3 mL) were combined in an open vial along with a magnetic stir bar. The mixture was stirred at 130 °C for 30 minutes. After cooling to room temperature, the crude oil was transferred to a round bottom flask and reduced under vacuum to minimum volume. The product was purified using flash chromatography on silica gel with 2:8 ethyl acetate:hexanes as the mobile phase. R_f = 0.22. Yield: 2.01 g (96 %) of a yellow solid.

ESCI MS 315.1000 $(M\text{-}Na)^+$. Elemental analysis calculated for $C_{19}H_{16}O_3$: C, 78.06%; H, 5.52%; O, 16.42. Found: C, 78.35%; H, 5.52%, O, 16.13%.

^{1}H NMR (400 MHz, $(CD_3)_2SO$, RT): δ 8.70 (s, 1H), 8.35 (d, *J* = 8.9 Hz, 2H), 8.14 (d, *J* = 8.2 Hz, 2H), 7.62 (m, 2H), 7.56, (m, 2H), 6.16 (s, 2H), 3.63 (s, 2H), 2.10 (s, 3H). ^{13}C {^{1}H} NMR (140 MHz, $(CD_3)_2SO$): δ 201.5, 167.4, 130.9, 130.5, 129.0, 129.0, 126.8, 126.0, 125.3, 124.0, 59.9, 49.6, 30.0.

Polymer sample **P7**:

PDMS-NH_2 (1 g) and 9-anthracene-methylacetoacetate (0.146 g, 25 equivalents) were combined in a vial with 2 mL of THF. The system was sonicated until homogeneous, and then heated in an oil bath at 70 °C until the THF had been removed (approximately 1 hour). The vial was stoppered and an N_2 inlet was added. The system was heated at 100 °C for 18 hours under a constant flow of N_2 to afford the product as a yellow oil without further purification. The resulting oil was fully miscible with CH_2Cl_2 and THF. Samples **P3** and **P25** were prepared using the same procedure, changing only the moles of **AnAc** added.

^{1}H NMR (peaks resulting from polymer backbone have been omitted for clarity) (400 MHz, CD_2Cl_2, RT): δ 8.72 (s, 1H), 8.49 (s, 1H), 8.38 (m, 2H), 8.03 (m, 2H), 7.51 (m, 4H), 6.06 (s, 2H), 4.38 (s, 1H), 3.22 (m, 2H), 1.88 s, 3H), 1.65 (m, 2H), 0.60 (m, 2H)

Polymer **PDMS-NH2**:

^{1}H NMR (400 MHz, CD_2Cl_2, RT): δ 2.62 (m, 2H), 1.46 (m, 2H), 0.51 (m, 2H), 0.09 (s, 97H)

Thin Films:

20 wt % Solutions of polymer were prepared using CH_2Cl_2. Solutions were dropcast (≈ 70 µL) directly onto glass slides and allowed to air dry. Irradiation on thin films was carried out using a UVGL-58 6W handheld UV lamp at a distance of 3 cm, irradiating through a Pyrex watch glass to cut-off any light below 300 nm. The soluble fraction of thin films was determined by immersing a pre-weighed sample in 100 mL of CH_2Cl_2 for 24 hours. Then, the sample was removed, rinsed thoroughly with clean CH_2Cl_2, and dried under vacuum for 24 hours. The weight of the dried mass was used to calculate the percent of mass that was soluble. Bulk samples were irradiated using a Rayonet photoreactor equipped with ten 365 nm 35W bulbs.

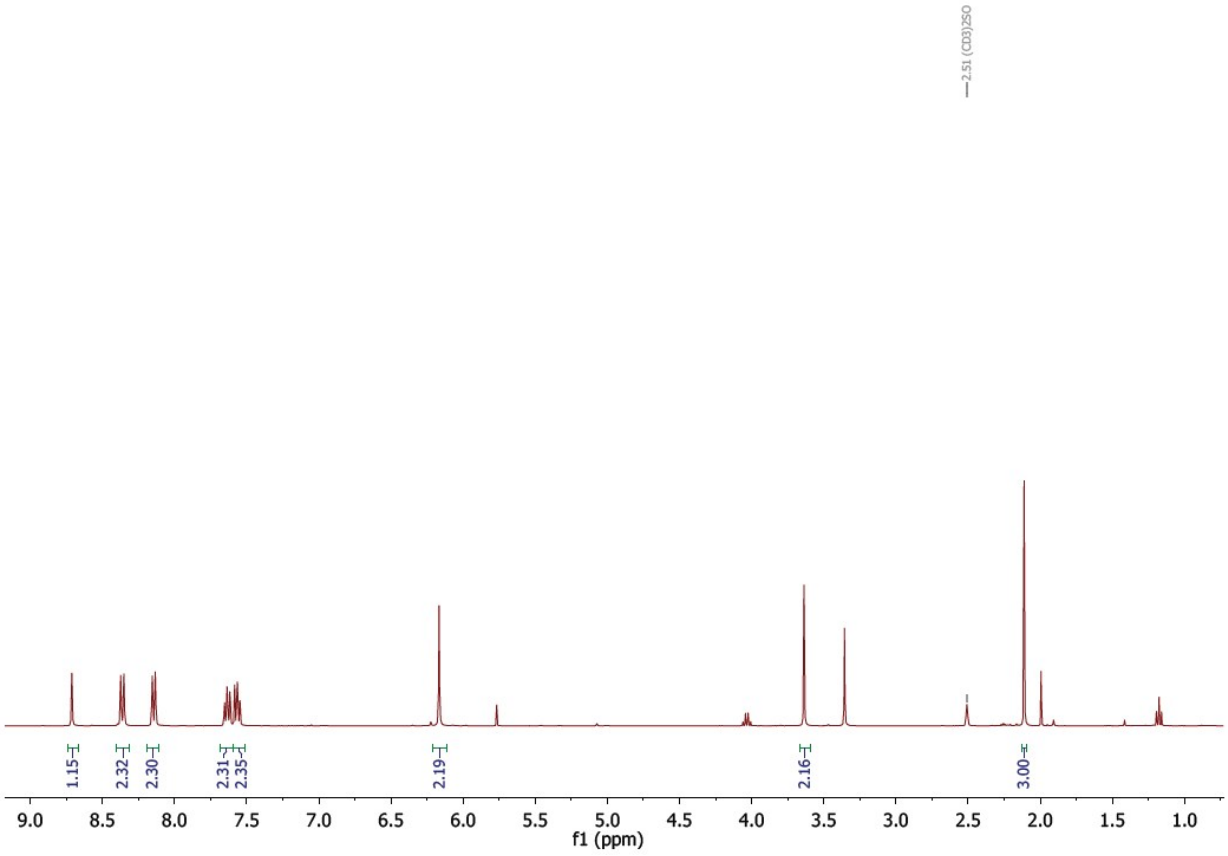

Figure S1. ^{1}H NMR spectrum of **AnAc**. 400 MHz, RT, $(CD_3)_2SO$. Other peaks are residual solvent peaks.

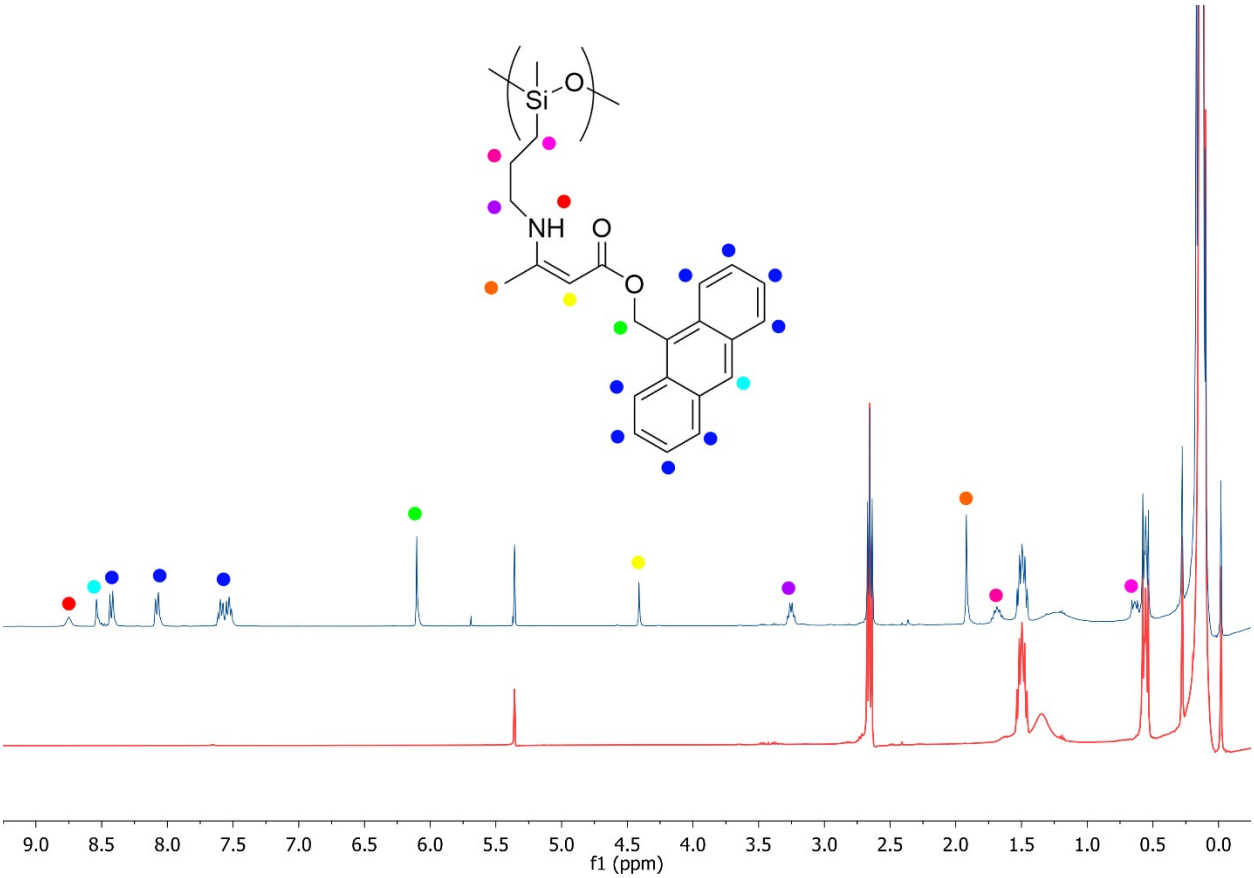

Figure S2. ^{1}H NMR spectra of (bottom) **PDMS-NH$_2$** and (top) **P7** showing the new peaks due to **AnAc** condensation. 400 MHz, RT, CD_2Cl_2

ppm	D_t x10^{-11} (m^2/s)	ID
8.542	**1.182**	**Anthracene C-H**
8.447	**1.152**	**Anthracene C-H**
8.075	**1.152**	**Anthracene C-H**
7542	**1.158**	**Anthracene C-H**
4.447	**1.190**	**RC=CH-CO2R**
2.69	**1.199**	**Non-condensed propylamine**
0.167	**1.099**	**Si-CH$_3$**

Table S1. Calculated translational diffusion coefficients for ^{1}H NMR peaks corresponding to the anthracene portion, vinylogous urethane, and **PDMS-NH2** chain, demonstrating that all components diffuse at similar speeds. D_t determined from 2D DOSY measurements, 400 MHz, RT, CD_2Cl_2.

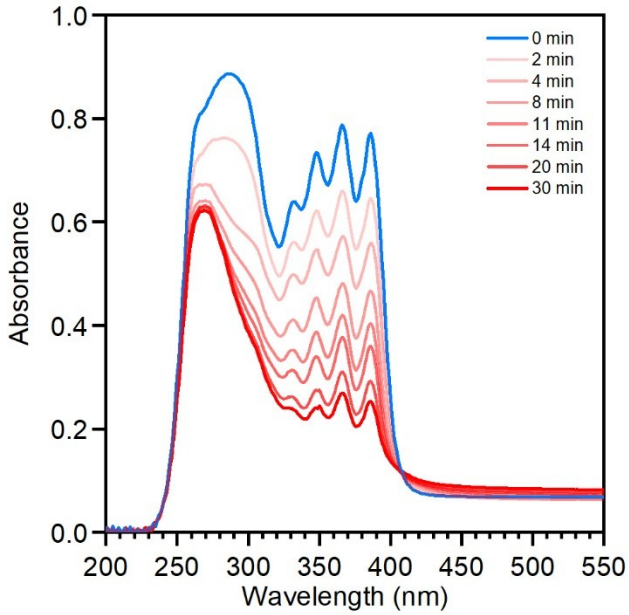

Figure S3. UV-VIS spectra of a dropcast sample of polymer **P7** as a function of irradiation time using 365 nm irradiation.

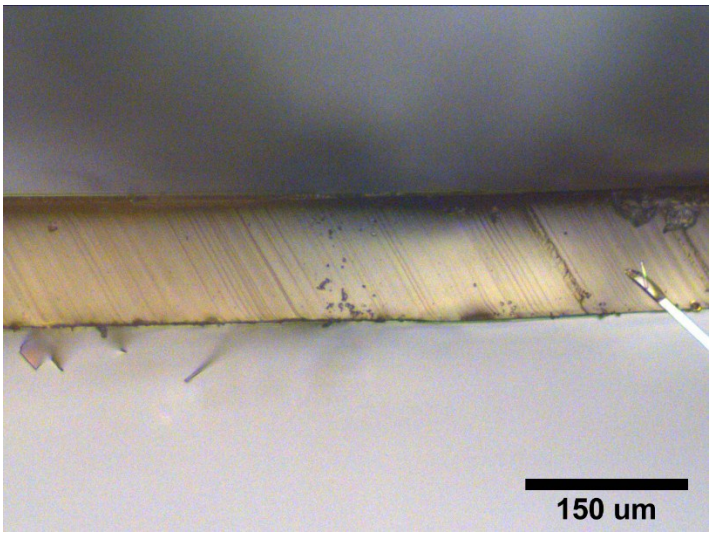

Figure S4. Optical microscope image of a side-on view of a free-standing piece of irradiated **P7**, showing the approximate film thickness of 115 µm.

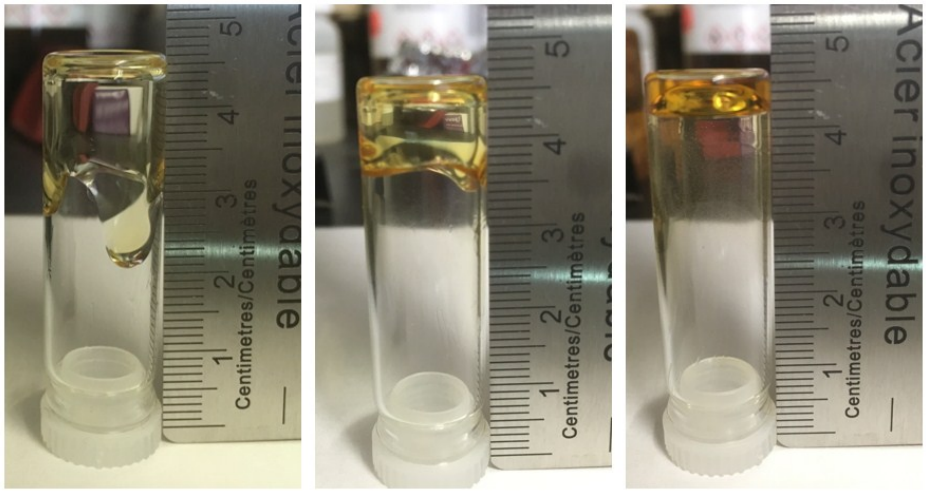

Figure S5. Average approximate distance (d) travelled by a sample of polymer **P25** two minutes after inversion as a function of irradiation time (t).

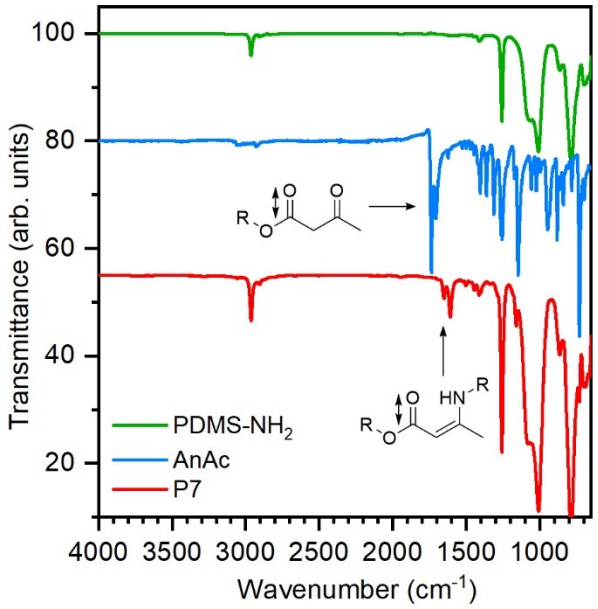

Figure S6. FT-IR spectrum of polymer **P7**, condensed from **AnAc** and **PDMS-NH2**. Arrows indicate the C=O stretch before (blue) and after condensation (red), showing a shift to lower wavenumbers resulting from increased conjugation. No changes were observed in **P7** after irradiation.

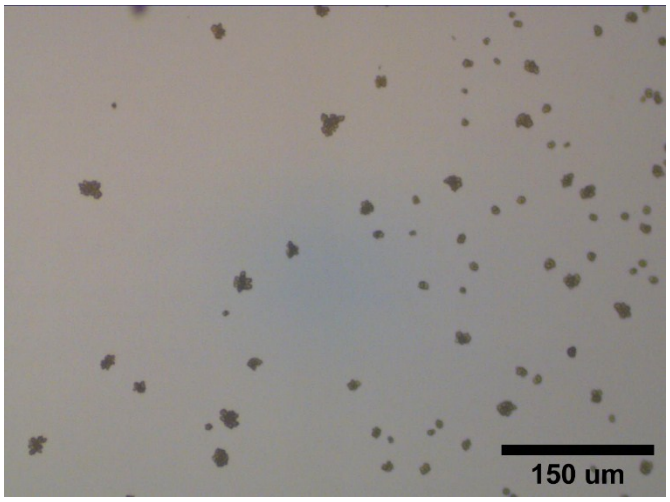

Figure S7. Optical microscope image of a thin film of **P7** after 15 minutes of 365 nm irradiation showing only spherical crystalline seeds.

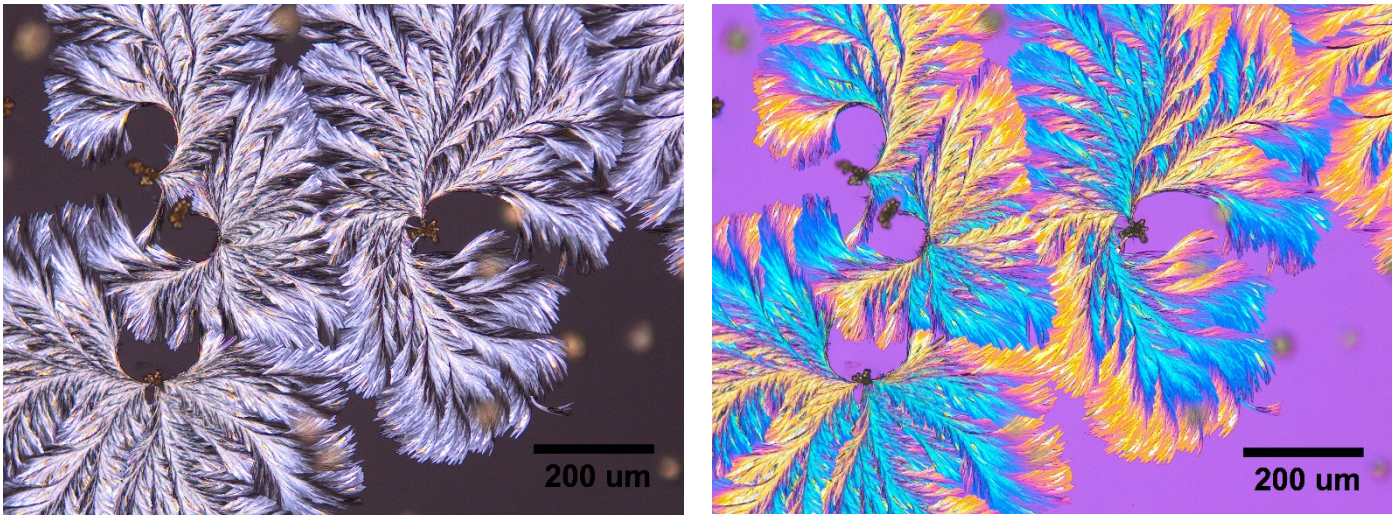

Figure S8. Optical microscope image of **P7** leaves under a cross-polarizer (left) and cross-polarizer + 530 nm retardation plate (right) showing crystal structures having grown into each other without merging.

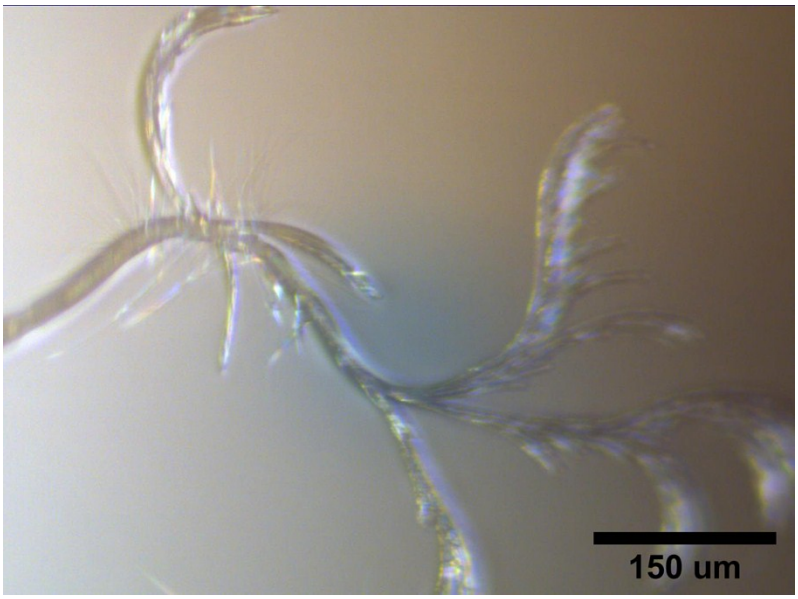

Figure S9. Optical microscope image of bulk **P7** in a vial after one hour of isotropic 365 nm irradiation, imaged through the sides of the glass vial.

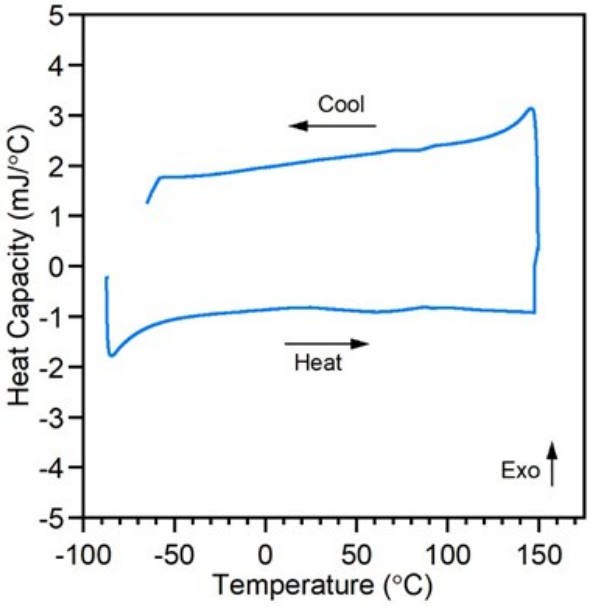

Figure S10. Differential scanning calorimetry of **P7** after 60 minutes of irradiation, showing a full heating and cooling cycle with a temperature ramp speed of 10°C/min.

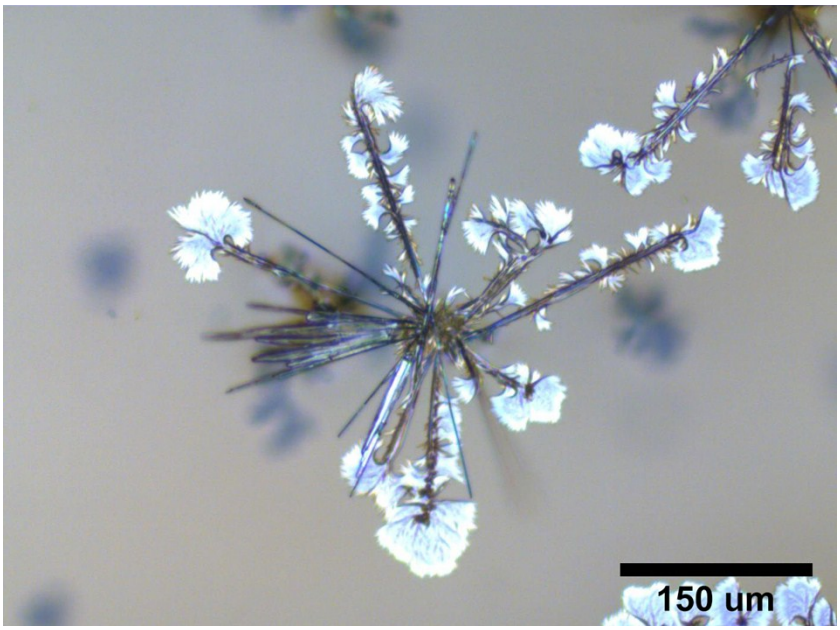

Figure S11. Optical microscope image of a thin film of **P7** after 60 minutes of 365 nm followed by 60 minutes at 100 °C.

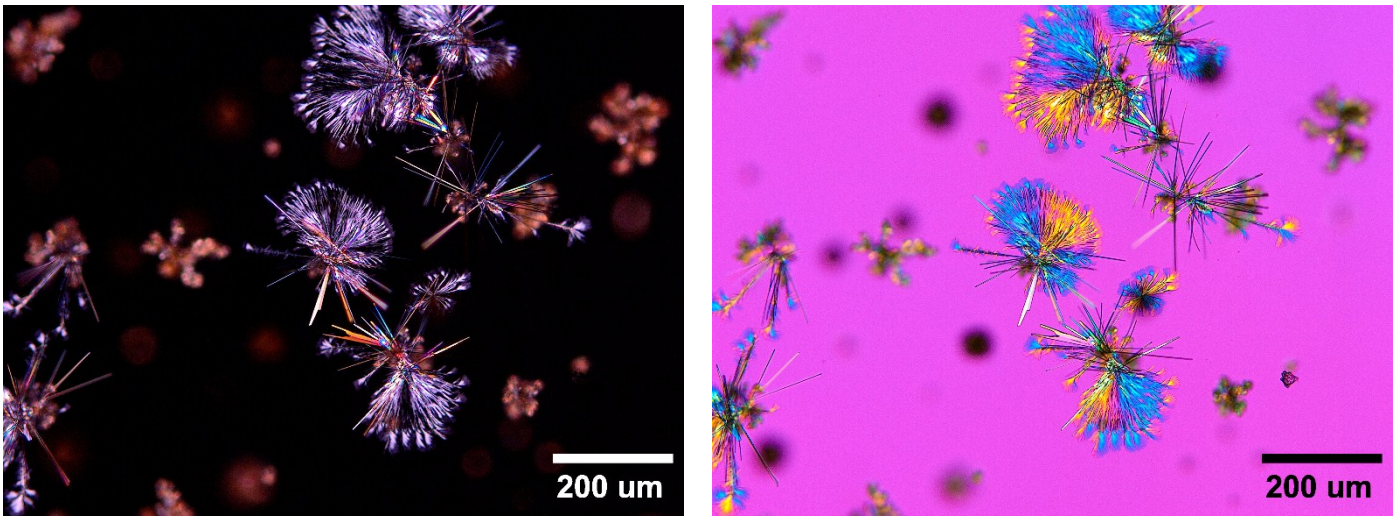

Figure S12. Optical microscope image of **P7** leaves after 60 minutes at 100 °C under a cross-polarizer (left) and cross-polarizer + 530 nm retardation plate (right).

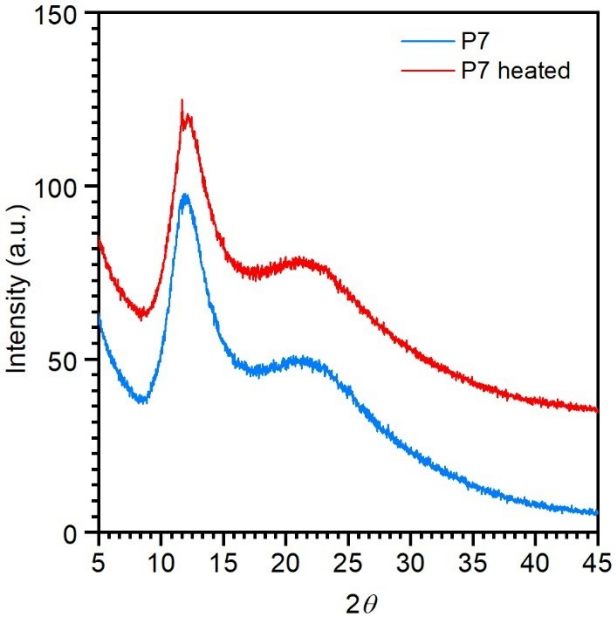

Figure S13. PXRD measurements of crystallized **P7** and crystallized **P7** after 1 hour at 100 °C. Cu radiation, RT.

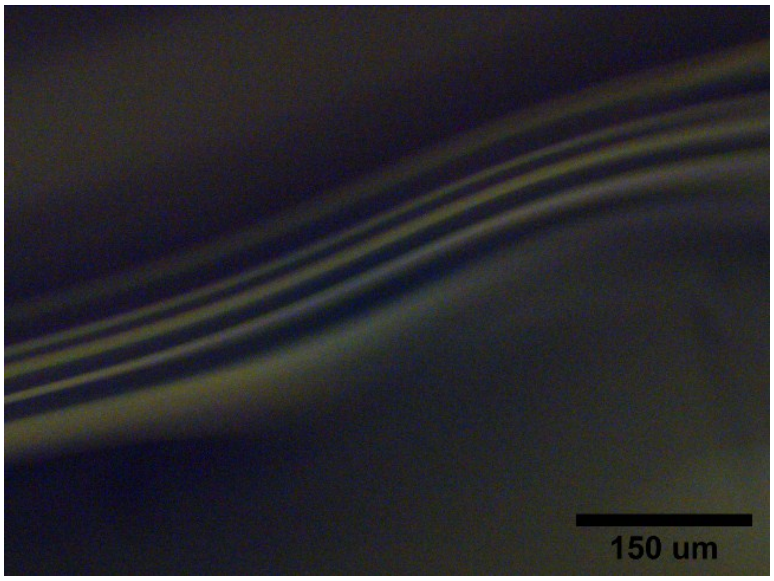

Figure S14. Optical microscope image of the center of **P25** after ten minutes of irradiation showing buckling of the surface.

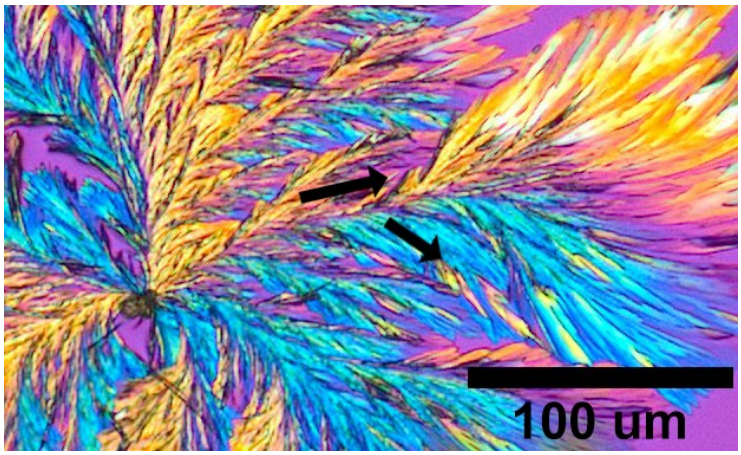

Figure S15. Magnified POM image from Figure 1f with arrows showing 45° branching of the blue region from the radial orange branch.

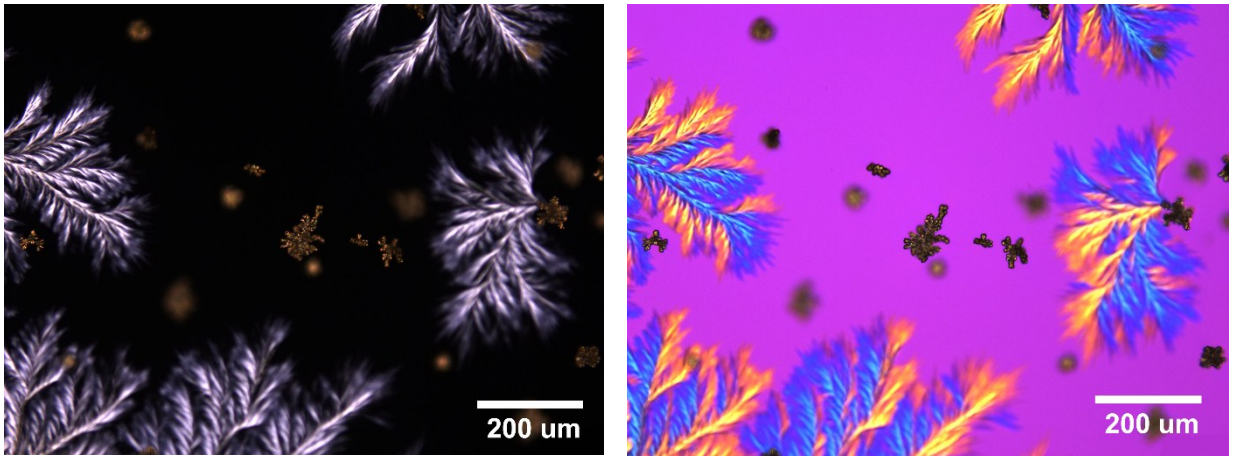

Figure S16. Optical microscope image of **P7** seeds under a cross-polarizer (left) and cross-polarizer + 530 nm retardation plate (right).

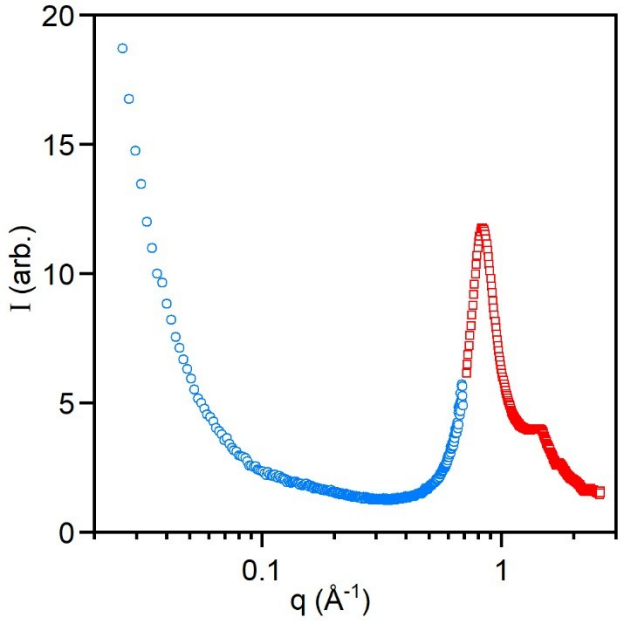

Figure S17. Wide-angle x-ray scattering and small-angle x-ray scattering of a free-standing **P7** film after irradiation, showing only two diffuse peaks attributed to the PDMS backbone. Measurements were focused on areas containing crystalline leaves.

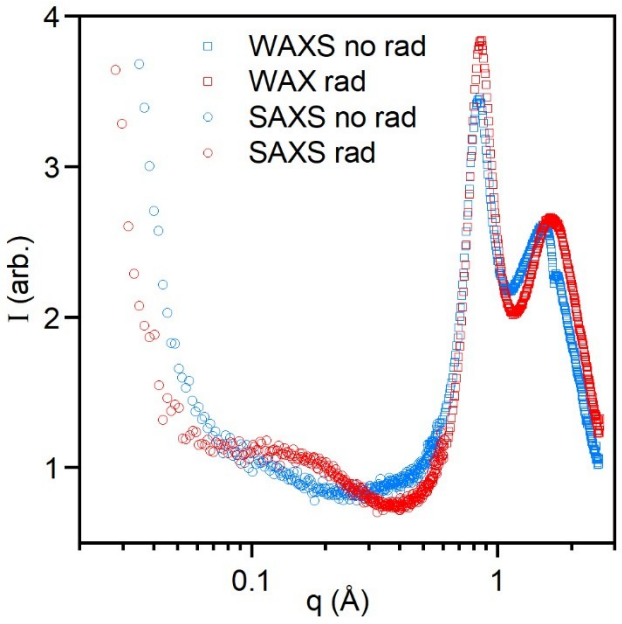

Figure S18. WAXS and SAXS of P7 in a glass capillary, before irradiation and after 120 minutes of 365 nm irradiation.

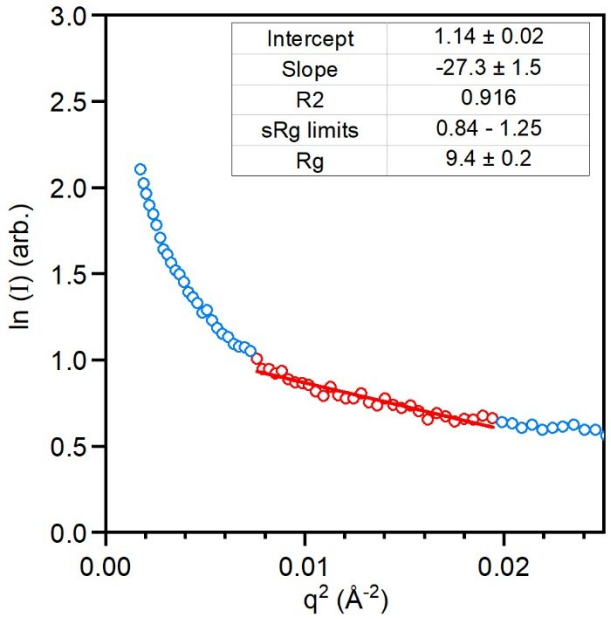

Figure S19. Guinier plots of the low q region of the SAXS spectrum of crystallized **P7**, focused on the crystalline regions.

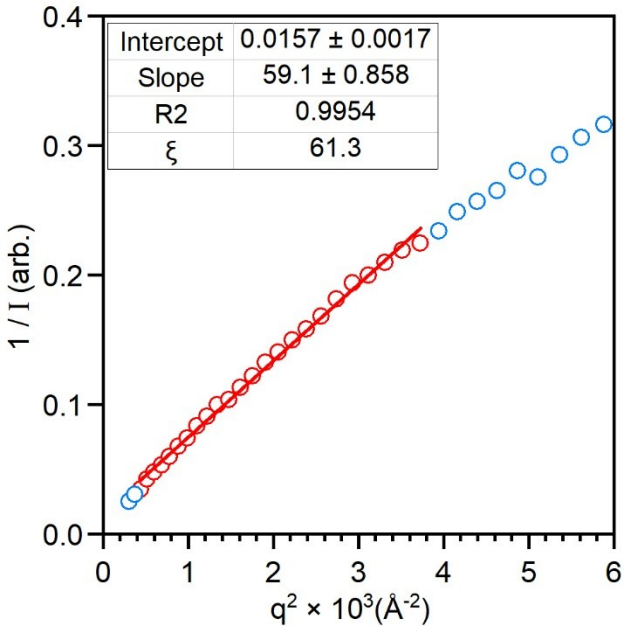

Figure S20. Ornstein-Zernike plot of crystallized **P7** giving a correlation distance of 61 Å.

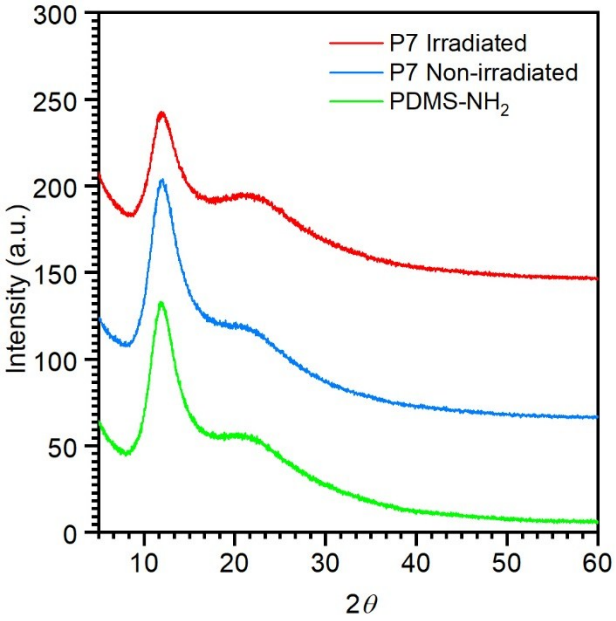

Figure S21. PXRD measurements of **P7** before irradiation, after 60 minutes of 365 nm irradiation, and of **PDMS-NH_2**. Cu radiation, RT.

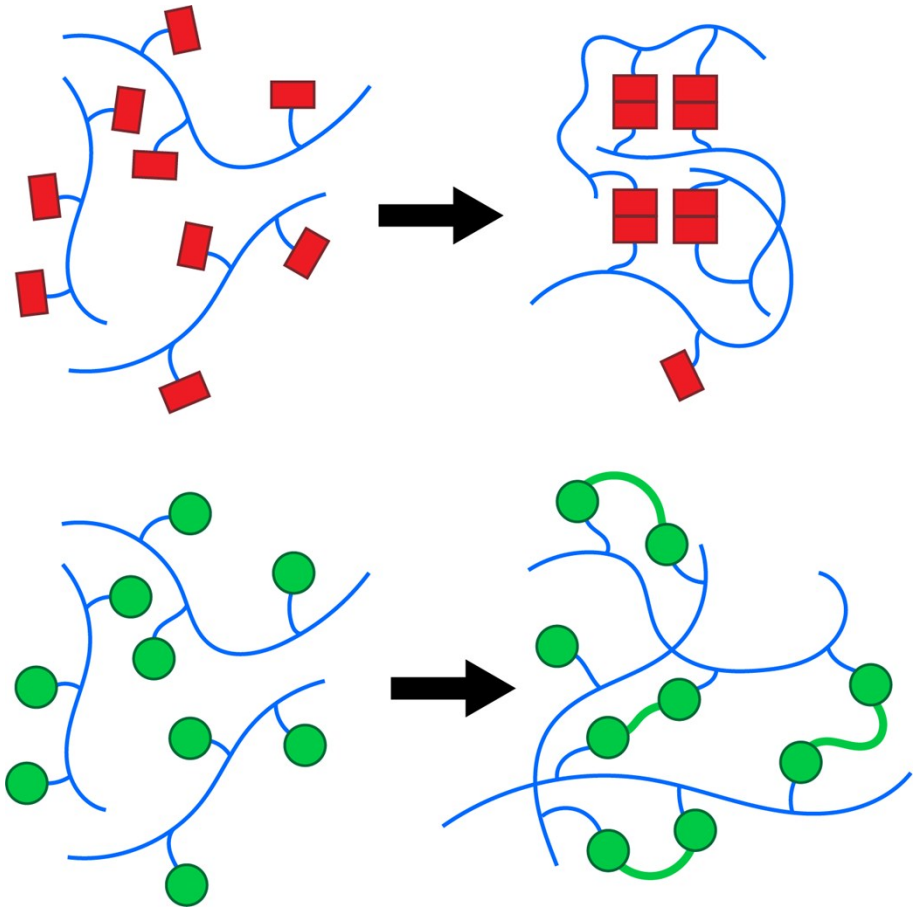

Figure S22. Schematic representation of (top) crosslinking via anthracene dimerization resulting in oriented crosslinked areas surrounded by amorphous polymer chains and (bottom) crosslinking via a flexible, non-rigid moiety resulting in no ordering.

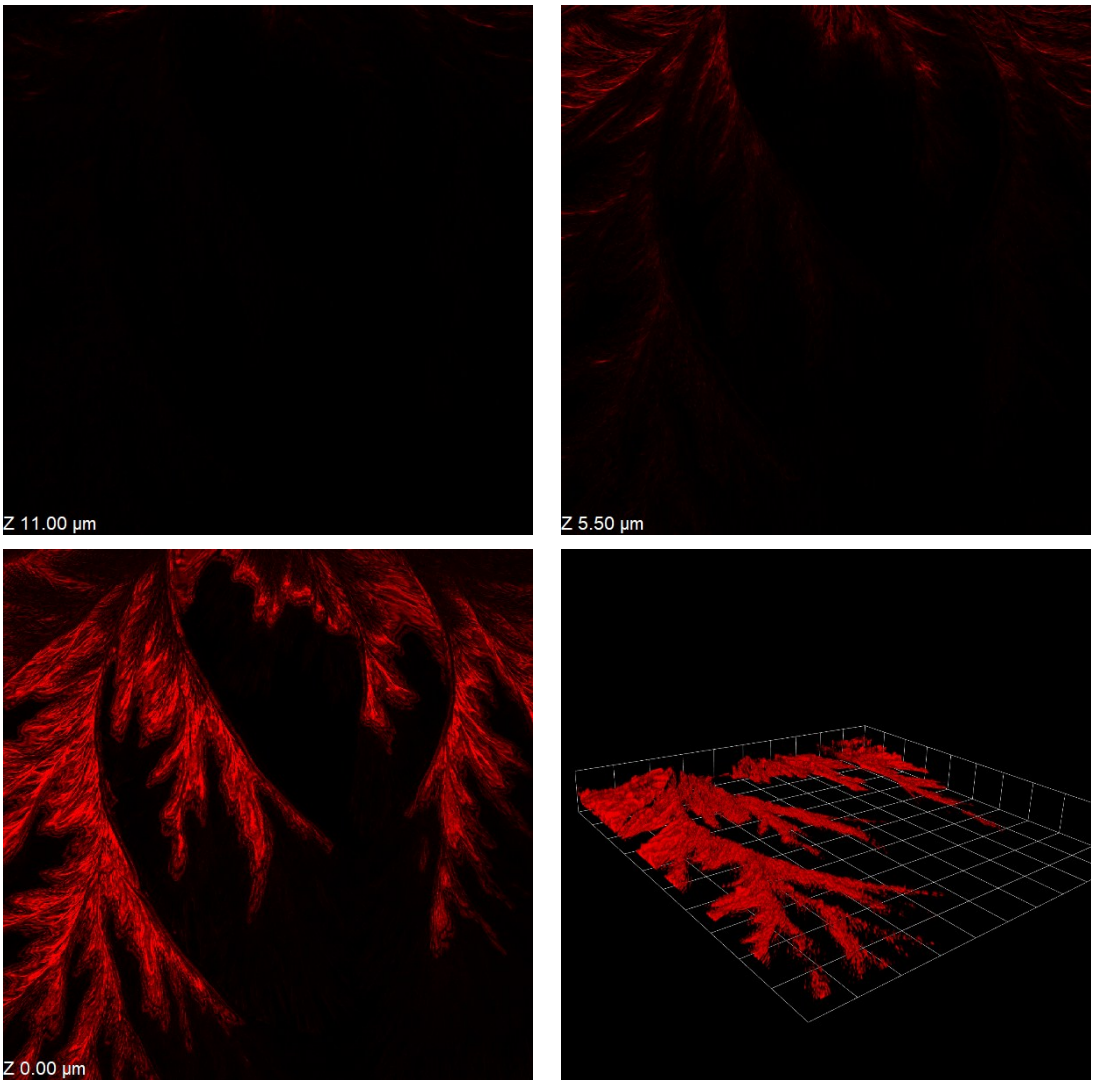

Figure S23. Confocal microscopy images of **P7** leaf edges at different depths and inverted 3D reconstructed data. Inset numbers are the vertical distance from the surface. Reconstruction boxes are 60 µm × 60 µm.

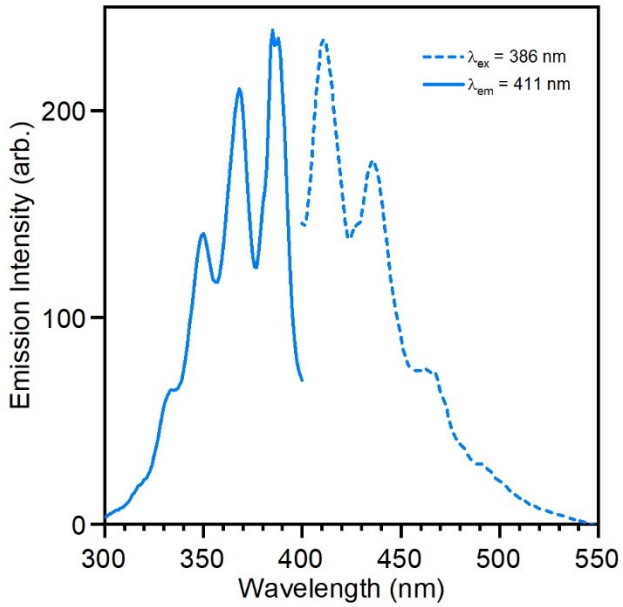

Figure S24. Excitation and emission spectrum of a thin film of **P7** after one hour of 365 nm irradiation.

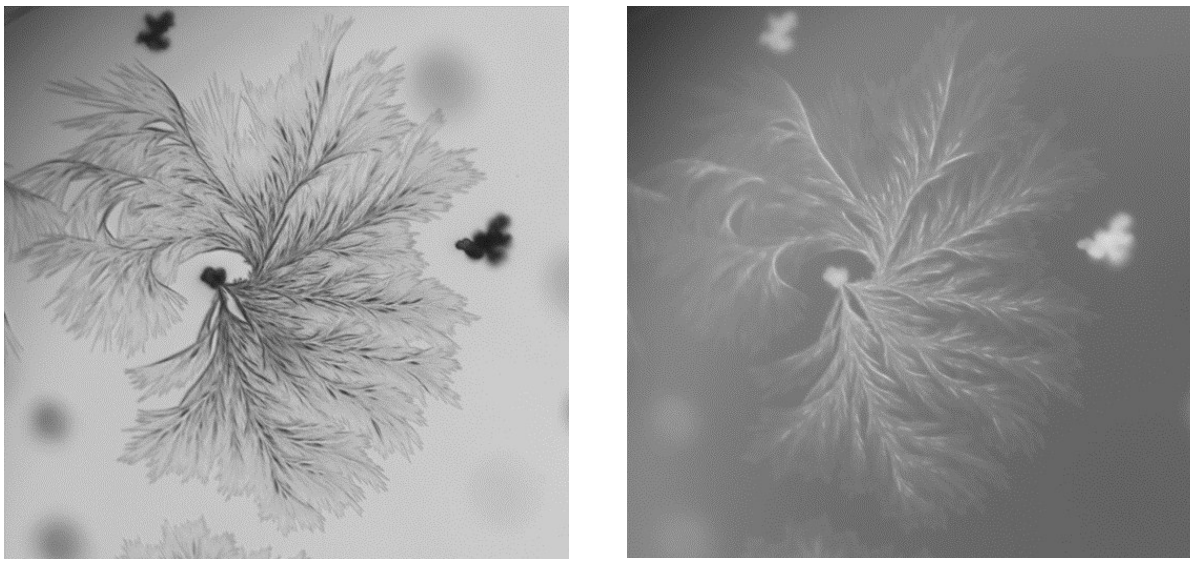

Figure S25. (Left) Bright field and (right) fluorescence imaging of **P7** crystals at 10× magnification, using 350 nm excitation light.

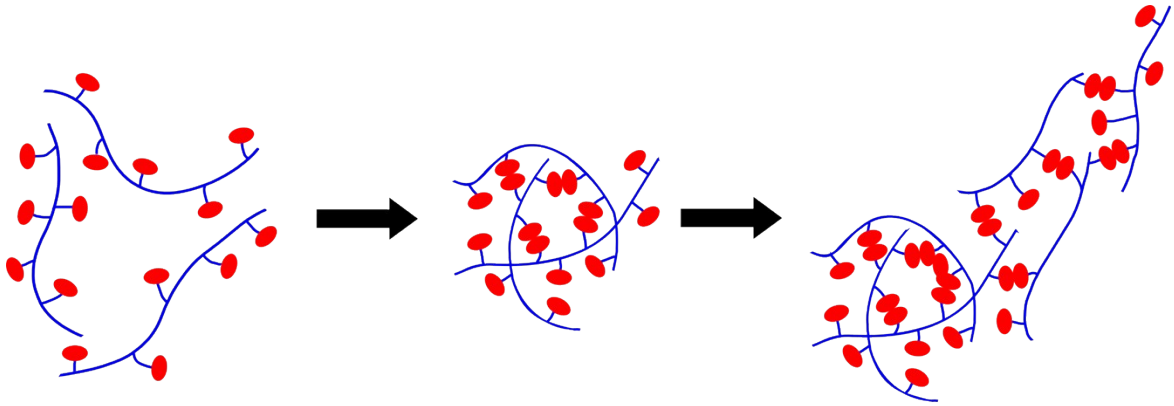

Figure S26. Schematic representation for confinement of anthracene molecules in the crystalline seeds and leaves giving rise to the fluorescence images from Figure S24, proceeding from linear polymer to seed to leaf growth.

Sample ID	D_t (cm^2/sec)	T_1 (ms)	T_2 (ms)	T_1/T_2
PDMS-NH2	4.85×10^{-7}	0.815	421	1.94
P3	8.56×10^{-9}	1.067	161	6.61
P7	7.60×10^{-9}	0.9599	74	12.92
P25	9.30×10^{-9}	1.1537	41	27.85
P7 crystalline	6.20×10^{-10}			

Table S2. Translational diffusion speeds, T_1, and T_2 values for liquid polymer samples and crystallized **P7**, measured using PFG ^{1}H NMR.

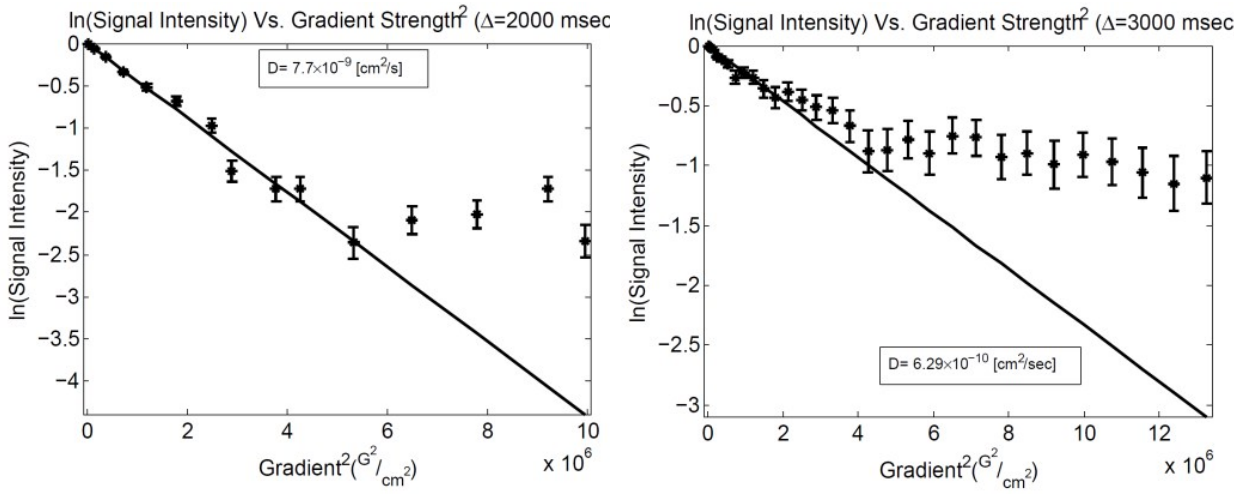

Figure S27. PFG ^{1}H NMR diffusion measurement. The same data as in Figure 4, plotted as the natural logarithm of the signal intensity vs. the gradient strength squared to linearize the Gaussian behaviour of the Stejskal – Tanner diffusion equation. Liquid **P7** (left) and irradiated **P7** (right). In the liquid sample there appears to be an abrupt transition between single-component diffusion and a small (~10%), much slower diffusing component. The irradiated sample appears to make a more gradual transition, suggesting a distribution of slower diffusion coefficients. Larger error bars for the irradiated sample reflect the lower signal to noise ratio due to the slower diffusion rates and faster T_2 decay.

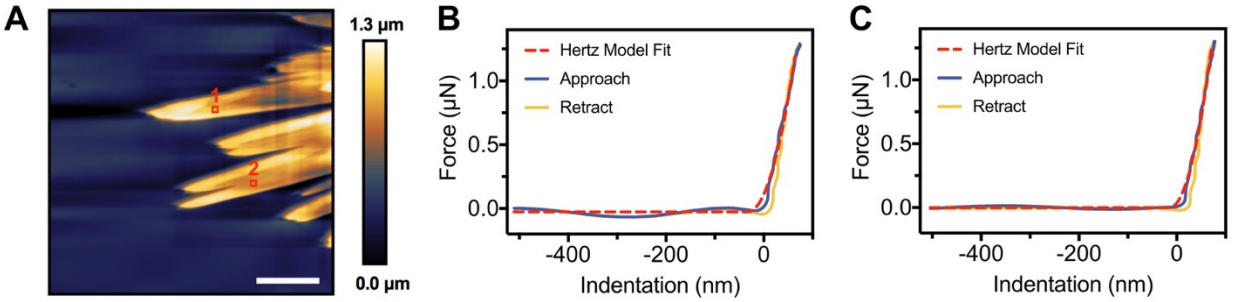

Figure S28. (**a**) AFM height image of crystallized **P7**, scale bar = 8 µm. (**b**) Representative force indentation curve taken at point 1. (**c**) Representative force indentation curve taken at point 2.

Reference

(1) Michal, C. A.; Broughton, K.; Hansen, E. A high performance digital receiver for home-built nuclear magnetic resonance spectrometers. *Rev. Sci. Instrum.* 2002, **73**, 453.